MAURIZIO DAPOR

ELECTRON-BEAM PENETRATION IN SURFACE FILMS

ABSTRACT - DAPOR M., 2005 - Electron-beam penetration in surface films.

Atti Acc. Rov. Agiati, a. 255, 2005, ser. VIII, vol. V, B: 47-57.

In electron microscopy an electron-beam impinges on a solid target. Each individual electron loses energy and changes its direction of motion due to atomic electron excitation, plasmon emission and interactions with the nuclei of the medium. The travel of the electron in the solid may be described by the inelastic scattering processes – due to the interaction between the incident electron and the atomic electrons – and the elastic scattering processes – due to the collisions between the incident electron and the nuclei. Once calculated the electron inelastic and elastic scattering cross sections, it is possible to deal with the problem of the interaction of an electron-beam with a solid by use of the Monte Carlo method, a statistical tool able to solve mathematical problems. This work is focused on the simulation of the interaction of an electron-beam with solid targets constituted by Au thin films deposited on Al substrates. The Monte Carlo simulation results are used to predict the beam behavior: the implantation profiles are utilized, in particular, to calculate the ranges of penetration in the Au/Al system. An analytical model to calculate the maximum range of penetration of electrons in the Au/Al system is proposed.

KEY WORDS - Monte Carlo method, Electron-beam interactions with solids, Electron microscopy.

RIASSUNTO - DAPOR M., 2005 - Penetrazione di fasci di elettroni in strati superficiali.

In microscopia elettronica un fascio di elettroni viene inviato contro un bersaglio solido. Ogni elettrone del fascio perde energia e cambia direzione ad ogni collisione a causa dell'eccitazione degli elettroni atomici, dell'emissione di plasmoni e delle interazioni con i nuclei atomici del bersaglio. La traiettoria dell'elettrone nel solido può essere descritta mediante i processi di diffusione anelastica – dovuti all'interazione tra l'elettrone incidente e gli elettroni atomici – ed i processi di diffusione elastica – causati dalle collisioni dell'elettrone incidente con i nuclei atomici. Una volta calcolate le sezioni d'urto anelastica ed elastica, è possibile trattare il problema dell'interazione di fasci di elettroni con bersagli solidi usando il metodo di Monte Carlo, uno strumento statistico che permette di risolvere problemi matematici. Il presente lavoro è focalizzato sulla simulazione dell'interazione di un fascio di elettroni con bersagli solidi co-

stituiti da strati sottili d'oro depositati su substrati di alluminio. I risultati della simulazione di Monte Carlo sono usati per predire il comportamento del fascio di elettroni: in particolare si utilizzano i profili di impianto per calcolare la profondità di penetrazione degli elettroni nel sistema Au/Al. Viene proposto un modello analitico per calcolare il massimo range di penetrazione nel sistema Au/Al.

PAROLE CHIAVE - Metodo di Monte Carlo, Interazioni di fasci di elettroni con solidi, Microscopia elettronica.

1 INTRODUCTION

Let us consider an electron (or a positron) stream with energy E_0 incident on a homogeneous target (bulk, unsupported thin film, surface film) in the $+z$ direction. Many scientific works can be found in the literature dedicated to the problem of calculating the electron-beam (positron-beam) behavior inside solid targets and the related phenomena: for a list of papers that have dealt, in the recent years, with the problem from various points of view see, for example, [1-17].

Each particle can be both elastically scattered by collisions with the atomic nuclei and undergo inelastic interactions by losing energy essentially by collisions with the atomic electrons and by plasmon excitations. In the Monte Carlo scheme utilized in this work [18-22], the incident particles are assumed to lose energy with continuity inside the solid, the energy loss processes being all incorporated in the stopping power. The present Monte Carlo code uses the dielectric function approach proposed by Ashley [23] for the numerical evaluation of the stopping power. Concerning the differential elastic scattering cross sections, necessary for the description of the electron-atom elastic collisions, they are calculated by the Quantum Relativistic Partial Wave Expansion Method (QRPWEM): for the differential elastic scattering cross section calculations see, for example, [24-27].

After a short description, in the next section, of the physical quantities involved and of the Monte Carlo code utilized, the following section is dedicated to the description of an analytical approach for the computation of the maximum range of penetration for supported thin films. Then the Monte Carlo results concerning the depth distributions are shown. Monte Carlo data about the maximum range of penetration are compared to the proposed analytical calculations.

2 SUPPORTED AND UNSUPPORTED THIN FILMS

2.1 Absorption, backscattering, and transmission

Let us consider a solid of a given thickness and of a given material. We indicate with R the maximum penetration range and consider the target as a film if its thickness t is lower than R and a bulk for t greater than R. When $t \geq R$, the fraction of particles transmitted is zero while the fraction of particles backscattered is equal to r, the so-called backscattering coefficient, i.e. the fraction of the primary beam backscattered by a bulk. Both R and r depend on the target atomic number, the beam energy and the kind of particles.

When $t \leq R$, the particle beam is split by the target in three different fractions which we indicate with η_A, η_B and η_T and represent, respectively, the fractions of particles absorbed, backscattered and transmitted. Each of them lies in the range [0,1]. The conservation of the total number of particles entails that, for a given thickness t,

$$\eta_A(t) + \eta_B(t) + \eta_T(t) = 1. \tag{1}$$

We have reserved the symbol ζ_A, ζ_B and ζ_T for the same fractions when the thin film is deposited on a substrate constituted of a different material.

Even for the ζ fractions, of course, the conservation of the total number of particles holds and, as a consequence,

$$\zeta_A(t) + \zeta_B(t) + \zeta_T(t) = 1. \tag{2}$$

Due to backscattering from the substrate, for any given film thickness t, $\zeta_B(t) \geq \eta_B(t)$ and $\zeta_T(t) \leq \eta_T(t)$.

Let be F the material constituting the film and S the material constituting the substrate. We use the subscripts F and S to indicate the material considered. For example, R_F and R_S represent the maximum penetration ranges in F and in S, respectively.

We assume that the thickness of the substrate is larger than the maximum penetration range R. In other words, for the primary energy considered, the double layer structure is a bulk target.

2.2 The Monte Carlo code

Let us adopt spherical coordinates (r, θ, ϕ) and assume that a stream

of mono-energetic electrons irradiates a solid target in the $+z$ direction. The path-length distribution is assumed to follow a Poisson-type law. The step-length Δl is then given by

$$\Delta l = -\lambda \ln (rnd_1), \tag{3}$$

where rnd_1 is a random number uniformly distributed in the range [0,1] and λ is the total elastic mean free path calculated by using the Quantum Relativistic Partial Wave Expansion Method (QRPWEM). The energy loss ΔE along the segment of trajectory Δl is approximated by

$$\Delta E = (dE/dl)\, \Delta l, \tag{4}$$

where $-dE/dl$ *is* the Ashley's stopping power [23].

The polar scattering angle θ after an elastic collision is calculated assuming that the probability $P(\theta)$ of elastic scattering into an angular range from 0 to θ, calculated by using the QRPWEM, is a random number rnd_2 uniformly distributed in the range [0,1]. The azimuth angle ϕ can take on any value in the range $[0,2\pi]$ selected by a random number rnd_3 uniformly distributed in that range.

Both the θ and ϕ angles are calculated relative to the last direction in which the particle was moving before the impact. The direction θ'_z in which the particle is moving after the last deflection, relative to the z direction, is given by

$$\cos \theta'_z = \cos \theta_z \cos \theta_z + \sin \theta_z \sin \theta_z \cos \phi, \tag{5}$$

where θ_z is the angle relative to the z direction before the impact.

The motion Δz along the z direction is then calculated by

$$\Delta z = \Delta l \cos \theta'_z. \tag{6}$$

The new angle θ'_z then becomes the incident angle θ_z for the next path length.

The particles are followed in their trajectories until their energies become lower than 50 eV or until they leave the solid target.

The Monte Carlo data presented in this paper have been obtained averaging, for each profile, on 4×10^6 electron trajectories.

3 SURFACE FILMS: MAXIMUM RANGE

3.1 Maximum range of electrons in solids

The mean path length traveled by an electron in a solid target of atomic number Z, when its energy reduces from E_0 to E, is given by

$$l(E_0, E, Z) = \int_0^l dl = \int_{E_0}^{E} \frac{dE}{dE/dl} \,. \tag{7}$$

This Equation allows us to calculate the maximum range of penetration,

$$R(E_0, Z) = \int_{E_0}^{E_{min}} \frac{dE}{dE/dl} \,, \tag{8}$$

where E_{min} is the energy at which an electron can be considered, for any practical purpose, absorbed in the target.

When the thickness of the target is greater than $R(E_0)$, the target is a bulk for the primary electron energy considered. On the other hand, when the thickness is lower than $R(E_0)$, the target is a film and, as already observed, the primary beam impinging on it is split into three fractions representing the absorbed, the backscattered, and the transmitted electrons.

3.2 The range-energy relationship

Using the data of stopping power obtained by a quantum mechanical treatment (the dielectric function approach described, for instance, by Ashley [23]), it is possible to show, for given energy ranges, that

$$-\frac{dE}{dl} = \frac{A}{E^q} \,. \tag{9}$$

If the energy is expressed in eV and the stopping power in eV/Å, in the energy range between 500 eV and 10,000 eV the best fit of the quantum mechanical stopping power for Al, for example, is given by

$$-\frac{dE}{dl} = \frac{124}{E^{0.60}} \,, \tag{10}$$

while, for Au, by

$$-\frac{dE}{dl} = \frac{154}{E^{0.48}}. \tag{11}$$

Using Equation (7),

$$l = \int_E^{E_0} \frac{E^q}{A}\, dE = \frac{1}{A(q+1)}(E_0^{q+1} - E^{q+1}). \tag{12}$$

With $E_{min} = 0$, we obtain

$$R(E_0, Z) = \frac{1}{A(q+1)} E_0^{q+1} \equiv K(Z) E_0^p, \tag{13}$$

where $p \equiv q + 1$ and

$$K(Z) \equiv \frac{1}{A(q+1)} = \frac{1}{Ap}. \tag{14}$$

Once defined

$$u \equiv \frac{l}{R} = 1 - \frac{E^p}{E_0^p}, \tag{15}$$

the range-energy relationship immediately follows:

$$E^p = (1-u)E_0^p. \tag{16}$$

3.3 Maximum range of penetration in systems composed by a surface film deposited on a bulk substrate

Let us now consider a system composed of a film of the material F of thickness t deposited on a substrate of the material S. Let us remind that the subscripts F and S will indicate the material considered. We assume that the thickness of the substrate is greater than R_S, namely the substrate is a bulk for the primary energy considered. We expect that the maximum penetration range R will be some combination of R_F and R_S depending on the film thickness: in particular, when $t \to 0$ then this combination will approach R_S and when $t \to R_F$ the combination approaches R_F. By Equation (13) it follows that

$$R(E, Z_F) \equiv R_F(E) = K_F E^{p_F}, \tag{17}$$

$$R(E, Z_S) \equiv R_S(E) = K_S E^{p_S}, \tag{18}$$

where $p_F = q_F + 1 \equiv q(Z_F) + 1$, $p_S = q_S + 1 \equiv q(Z_S) + 1$, $K_F \equiv K(Z_F)$, $K_S \equiv K(Z_S)$. Z_F and Z_S represent, respectively, the atomic numbers of the film and of the substrate. It is easy to see that, for $0 \le t \le R_F(E_0)$

$$R(E_0) = t + K_S \left(E_0^{p_F} - \frac{t}{K_F} \right)^{p_S/p_F}, \tag{19}$$

while, for $t > R_F$,

$$R(E_0) = R_F(E_0) = K_F E_0^{p_F}. \tag{20}$$

Indeed, for $t < R$,

$$R(E_0) = t + R_S(E), \tag{21}$$

where E is the mean energy of the beam after transmission through the film of thickness t. From the range-energy relationship, Equation (16), we can write that

$$E = \left(1 - \frac{t}{R_F(E_0)} \right)^{1/p_F} E_0 . \tag{22}$$

Now

$$R_S(E) = K_S E^{p_S} = K_S \left(1 - \frac{t}{K_F E_0^{p_F}} \right)^{p_S/p_F} E_0^{p_S} . \tag{23}$$

As a consequence

$$R(E_0) = t + K_S \left(E_0^{p_F} - \frac{t}{K_F} \right)^{p_S/p_F} . \tag{24}$$

Note that

$$\lim_{t \to 0} R(E_0) = K_S E_0^{p_S} = R_S(E_0) \tag{25}$$

and

$$\begin{aligned} &\lim_{t \to R_F(E_0)} R(E_0) \\ &= R_F(E_0) + K_S \left(E_0^{p_F} - \frac{K_F E_0^{p_F}}{K_F} \right)^{p_S/p_F} \\ &= R_F(E_0) . \end{aligned} \tag{26}$$

4 Results and discussion

The stopping profiles vs. the depth inside the solid are represented in Figure 1 for Al and in Figure 2 for Au. The stopping profiles were calculated for two primary energies, 5 and 10 keV. The integration of the curves, for each primary energy, gives the absorption coefficient $1 - r$, where r is the backscattering coefficient.

An example of depth profile of an electron-beam penetrating in a system composed by a thin film of Au deposited on a substrate of Al is presented in the Figure 3 for primary energy equal to 5 keV and film thickness equal to 200 Å.

From similar profiles it is possible to calculate the maximum ranges of penetration R. They are calculated looking for the first point, in each profile, for which $P(z) = 0$. The comparison between the results of the model represented by the Equation (24) and the Monte Carlo results concerning the maximum range of penetration as a function of the thickness are presented in Table 1 and in Table 2 (for 5 keV and 10 keV, respectively). The Monte Carlo data are slightly lower than the analytical data, due to the fact that Monte Carlo code takes into account also the elastic scattering. The differences between Monte Carlo and analytical results, for the thin films treated in this paper, are ~ 10 %.

Equation (24) is then a satisfactory approximation of the maximum range for thin films: it is a simple closed formula that allows one, from the knowledge of the stopping powers of the individual materials constituting the system (film and bulk), to quickly calculate the maximum penetration range with a quite good accuracy (~ 10 %).

5 Conclusion

The paper was focused on the simulation of the interaction of an electron-beam with solid targets constituted by thin films deposited on substrates. The Monte Carlo results were used to predict the beam behavior: the depth distributions have been used to calculate the range of penetration in the system. An analytical model to calculate the maximum range of penetration of electrons in the system has been proposed. The results of the closed formula about the maximum range proposed in this paper have been compared with the Monte Carlo data and satisfactory agreement has been found.

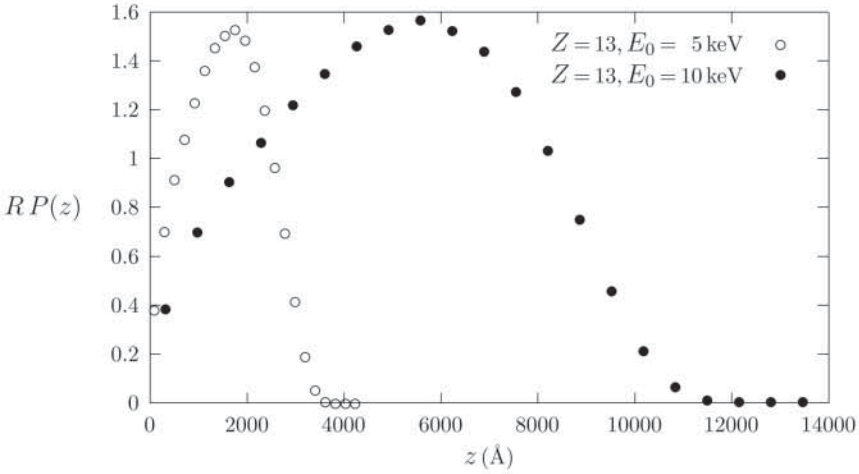

Fig. 1. Stopping profile $RP(z, E_0)$ vs. z (where R is the maximum range, $P(z, E_0)$ the depth distribution, z the depth inside the solid measured from the surface and E_0 the primary energy) for electrons in Al. For any given primary energy, integration of $P(z, E_0)$ from $z = 0$ to $z = R$ gives the absorption coefficient $1 - r$. The data presented concern Monte Carlo simulations of electron-beams irradiating targets in the $+z$ direction. ○: $E_0 = 5$ keV. ●: $E_0 = 10$ keV

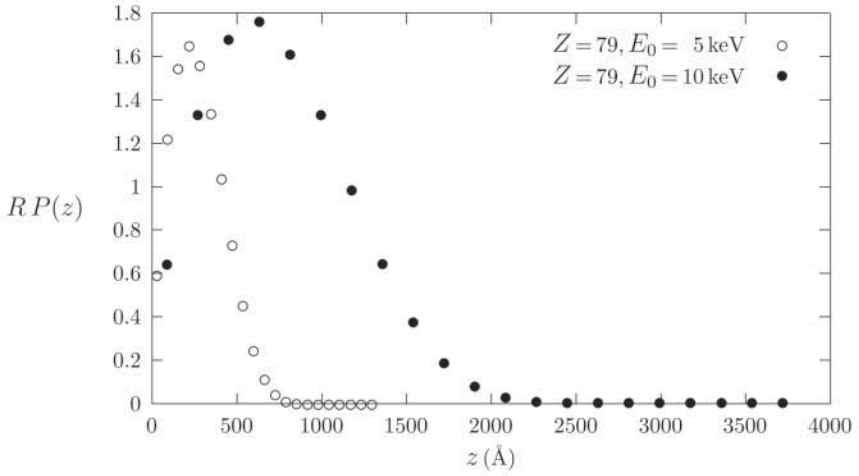

Fig. 2. Stopping profile $RP(z, E_0)$ vs. z (where R is the maximum range, $P(z, E_0)$ the depth distribution, z the depth inside the solid measured from the surface and E_0 the primary energy) for electrons in Au. For any given primary energy, integration of $P(z, E_0)$ from $z = 0$ to $z = R$ gives the absorption coefficient $1 - r$. The data presented concern Monte Carlo simulations of electron-beams irradiating targets in the $+z$ direction. ○: $E_0 = 5$ keV. ●: $E_0 = 10$ keV

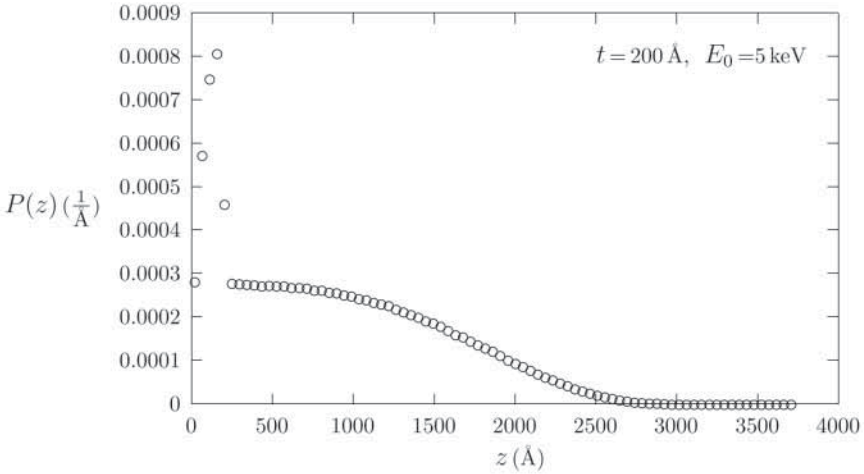

Fig. 3. Depth profile $P(z)$ of 5 keV electrons penetrating into a thin film of Au deposited on an Al substrate. The Au film thickness is 200 Å. Integration of $P(z)$ from $z = 0$ to $z =$ 200 Å gives the fraction of electrons absorbed by the surface film. Integration of $P(z)$ from $z = 200$ Å to $z = R$ gives the fraction of electrons transmitted through the surface film (and absorbed by the substrate). ○: Monte Carlo data

t (Å)	R (Å) Eq. (24)	R (Å) Monte Carlo
0	4176	3908
50	4054	3700
100	3932	3596
150	3811	3445
200	3691	3296
250	3571	3150

Tab. 1. Maximum range of 5 keV electron beams impinging on systems composed by films of Au deposited on Al substrates as a function of the film thickness.

t (Å)	R (Å) Eq. (24)	R (Å) Monte Carlo
0	12661	12244
250	11976	11634
500	11296	10728

Tab. 2. Maximum range of 10 keV electron beams impinging on systems composed by films of Au deposited on Al substrates as a function of the film thickness.

REFERENCES

[1] STAUB P.F. - J. PHYS. D: Appl. Phys. 27, 1533 (1994).

[2] BARÒ J., SEMPAU J., FERNÁNDEZ-VAREA J.M., SALVAT F. - Nucl. Instrum. Methods Phys. Res. B **100,** 31 (1995).

[3] MAGLEVANNY I., SMOLAR V. - Vacuum **46**, 1261 (1995).

[4] Vos M., Bottema M. - Phys. Rev. B **54,** 5946 (1996).

[5] LEE C.L., KONG K.Y., GONG H., ONG C.K. - Surf. Interface Anal. 24, 15 (1996).

[6] BUREK R., CHOCYK D. - Journal of Radioanalytical and Nuclear Chemistry **209,** 181 (1996).

[7] ASSA'D A.M.D., EL GOMATI M.M. - Scanning Microscopy **12,** 185 (1998).

[8] DAPOR M., MIOTELLO A., ZARI D. - Phys. Rev. B **61,** 5979 (2000).

[9] CHAOUI Z., BOUARISSA N. - Phys. Lett. A **297,** 432 (2002).

[10] BOUARISSA N., DEGHFEL B., BENTABET A. - Eur. Phys. J.: Appl. Phys. **19,** 89 (2002).

[11] STOIAN R., ROSENFELD A., ASHKENASI D., HERTEL I.V., BULGAKOVA N.M., CAMPBELL E.E.B. - Phys. Rev. Lett. **88**, 097603 (2002).

[12] COLEMAN P.G. - Appl. Surf. Sci **194,** 264 (2002).

[13] DEGHFEL B., BENTABET A., BOUARISSA N. - Phys. Stat. Sol. (b) **238,** 136 (2003)

[14] CHAOUI Z., BOUARISSA N. - J. Phys.: Condens. Matter **16,** 799 (2004).

[15] GLAZOV L.G., PÁZSIT I. - Nucl. Instrum. Methods Phys. Res. B **215,** 509 (2004)

[16] YADAV R.K., SHANKER R. - Phys. Rev. A **70,** 052901 (2004).

[17] CIMINO R., COLLINS I.R., FURMAN M.A., PIVI M., RUGGIERO F., RURNOLO G., ZIMMERRNANN F. - Phys. Rev. Lett. **93,** 014801 (2004).

[18] DAPOR M. - Eur. Phys. J.: Appl. Phys. **18,** 155 (2002).

[19] DAPOR M. - Nucl. Instrum. Methods Phys. Res. B **202,** 155 (2003).

[20] DAPOR M. - J. Appl. Phys. **95,** 718 (2004).

[21] DAPOR M. - Phys. Lett. A **333,** 457 (2004).

[22] DAPOR M. - Nucl. Instrum. Methods Phys. Res. B **228,** 337 (2005).

[23] ASHLEY J.C. - J. Electron. Spectrosc. Relat. Phenom. **46,** 199 (1988).

[24] DAPOR M. - J. Appl. Phys. **79,** 8406 (1996).

[25] SHI Q., FENG R., JI Q., WU S., ZHONG Z., XU K., LI J-M. - J. Phys. B: At. Mol. Opt. Phys. **30,** 5479 (1997).

[26] JABLONSKI A., SALVAT F., POWELL C.J. - J. Phys. Chem. Ref. Data 33, 409 (2004)

[27] DAPOR M. - Electron-Beam Interactions with Solids (Springer Tracts in Modern Physics) Springer-Verlag, Heidelberg, 2003.

Indirizzo dell'autore:
Maurizio Dapor - Istituto Trentino di Cultura. Centro per la Ricerca Scientifica e Tecnologica, Via Sommarive, 18 - I-38050 Povo, Trento, Italia.